Journal of Molecular Catalysis A: Chemical 355 (2012) 39–43

Contents lists available at SciVerse ScienceDirect

Journal of Molecular Catalysis A: Chemical

journal homepage: www.elsevier.com/locate/molcata

Editor's Choice paper

Size and shape dependent attachments of Au nanostructures to TiO_2 for optimum reactivity of Au–TiO_2 photocatalysis

Rupinder Kaur, Bonamali Pal*

School of Chemistry and Biochemistry, Thapar University, Patiala 147004, Punjab, India

ARTICLE INFO

Article history:
Received 9 September 2011
Received in revised form
23 November 2011
Accepted 24 November 2011
Available online 3 December 2011

Keywords:
Au co-catalysis
Au–TiO_2 photocatalysis
Transition metals catalysis
Au nanostructures attachment
Au nanocatalysts size and shape

ABSTRACT

This study demonstrated the effects of supported Au nanoparticles of various sizes and shapes on its co-catalytic activity imparted to TiO_2 during photocatalytic oxidation of salicylic acid. The TiO_2 photoactivity is remarkably improved with the decreasing size (9.5 ± 0.06 to 3.5 ± 0.25 nm) and increasing surface to volume (S/V) ratio (0.629–1.95 nm^{-1}) of spherical Au co-catalysts loading. The amount of Au (0.02 wt%) nanostructures supported to TiO_2 for its optimum photoreactivity is found to be 100 times less than the conventional prerequisite of 1–2 wt% metal photodeposition. The Au nanorod (aspect ratio = 2.8 ± 0.12 and S/V = 0.54 nm^{-1}) attachment to TiO_2 significantly decreased the photoactivity compared with the highly active quantum size (3.5 ± 0.25 nm) Au co-catalysts loading. The interaction of Au nanoparticles of various morphology with TiO_2 induces the photoexcited charge transfer process in varied extent, leading to diverse photocatalytic activity. Zeta potential (surface charge and conductance) measurement of aqueous dispersion of TiO_2, Au nanoparticles and salicylic acid was carried out to investigate the interaction among the various components in the photoreaction system.

1. Introduction

The deposition of transition metals [1–5] co-catalysts, Pt, Rh, Au, Cu and Ag onto TiO_2 catalyst usually improves the photocatalytic activity (PCA) which strongly depends on the extent, nature and the work function of the metals. Also, several strategies [3–11] have been employed to improve the PCA by tailoring size and shape of titania and metal nanostructure. After photoexcitation, the electron migrates to the metal where it gets trapped and e^-/h^+ recombination is reduced. The hole is then free to migrate to the surface where oxidation of the organics takes place. Conventional metal deposition techniques [9–14] generally lead to the growth of aggregated spherical particles and hence, the key effect of various sizes and shapes of metal nanoparticles (NPs) co-catalysts for photocatalytic reactions could not be determined. Metal NPs in the size regime 1–10 nm exhibit [15–17] characteristic size and shape dependent properties due to better charge transfer that cannot occur in bulk materials because the exposed surface atoms are 50 times less than quantum size particles [18]. Consequently, the size and shape specific activity of Au, Ag, Cu and Pt, NPs are studied [12–19] both as catalysts and co-catalysts for variety of thermal and photoreactions, respectively.

This size effect of metal NPs on the enhanced PCA of TiO_2 has been ascribed [20–24] to the Fermi energy shifts to the more negative direction for smaller NPs, leading to decrease the potential difference between the conduction band of TiO_2 and the Fermi level of the metal NPs. Hence, facilitates electron accumulation in the metal NPs and shifts the apparent Fermi level of metal NPs close to the bottom of the conduction band of TiO_2. As a result, Fermi level equilibrium takes place quickly and rapid electron transfer from TiO_2 to metal NPs occurs for improved photooxidation reaction by photoexcited hole. However, there have been very few comparative studies [22–26] in the literature on the use of specific metal NPs co-catalyst of unlike shapes and size dependent attachments on the PCA of TiO_2. Therefore, it is worth to study the Au–TiO_2 nanoassembly as a function of their interface geometry, the role of Au nanoparticles (AuNPs) morphology, their aggregation and spatial attachments effect compared to that of bare TiO_2. The loading of AuNPs, e.g., small nanosphere (SNS, size ≈ 3.5), medium size nanosphere (MNS, size > 5 nm), large nanosphere (LNS, size ≈ 9.5 nm), chemically aggregated nanosphere (ANS), nanorod (NR) and Au photodeposited particles (PAP), onto TiO_2 as shown in Scheme 1 (*MNS not shown here*) would alter the PCA of TiO_2 in different extent. Thus, the observed change in PCA could be attributed to the prevailing effect of size and shape dependent co-catalytic activity of AuNPs imparted to TiO_2. This is due to photoexcited charge transfer processess at the Au–TiO_2 interface which can be caused in photocatalytic test reaction.

* Corresponding author. Tel.: +91 175 2393443; fax: +91 175 2364498.
E-mail address: bpal@thapar.edu (B. Pal).

1381-1169/$ – see front matter © 2011 Elsevier B.V. All rights reserved.
doi:10.1016/j.molcata.2011.11.022

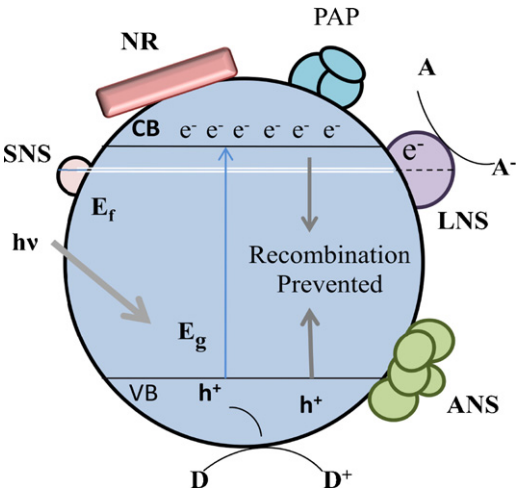

Scheme 1. Various morphology of Au nanoparticles-TiO_2 junctions.

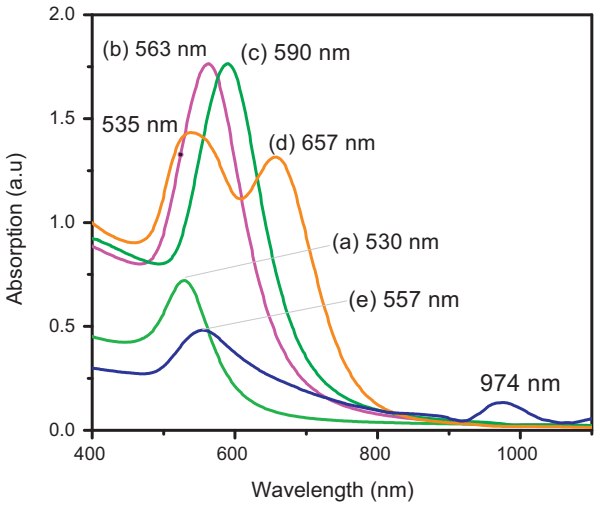

Fig. 1. Optical absorption spectra of various Au nanostructures showing different surface plasmon bands: (a) SNS (size ≈ 3.5 nm), (b) MNS (size > 5 nm), (c) LNS (size ≈ 9.5 nm), (d) NR (aspect ratio ≈ 2.8) and (e) ANS in methanol.

2. Experimental

The AuNPs of different sizes and shapes were synthesized [27–29] by seed-mediated approach in aqueous media at 0 °C. The Au seeds were first prepared by adding 250 μl (0.01 M) $HAuCl_4$ to 9.5 ml (0.1 M) cetyltrimethylammonium bromide (CTAB), followed by reduction with 600 μl (0.01 M) $NaBH_4$ solution under magnetic stirring for 2 min. The growth solution was prepared by treating a mixture of 500 μl (0.01 M) $HAuCl_4$, 9.5 ml (0.1 M) CTAB and 75 μl (0.01 M) $AgNO_3$ with 55 μl ascorbic acid (0.1 M). Then, 12 μl of above Au seed solution was introduced into the growth solution. Similarly, Au nanorod has been synthesized by the same seed approach method at 70 °C. The Au nanoparticles were repeatedly washed with deionized water under four cycles of centrifugation at 8500 rpm for 10 min and then used for photocatalytic reactions. Chemical aggregation of Au nanosphere [30,31] was carried out by the addition of 100 μl CH_3OH to 100 μl Au–MNS in a test tube and then the solvent was vacuum evaporated and used for photoreaction. For surface plasmon absorption study, the aggregation of the Au–MNS (SP band 563 nm and size > 5 nm) was carried out by direct addition of 1.5 ml CH_3OH (or CCl_4) to 1.5 ml of aqueous Au–MNS particles which showed 557 nm and 974 nm peaks.

The AuNPs are characterized by their surface plasmon (SP) band and TEM (Hitachi 7500, 200 kV) size and shape analysis. Photodeposition of 0.02 wt% Au onto TiO_2 (P25, Degussa, size ~20–30 nm) was carried out in a test tube using 5 ml deaerated aqueous suspension of CH_3OH, 50 mg TiO_2 and $HAuCl_4$ for 1 h light irradiation under stirring. The photoreaction was carried out in a test tube containing 5 ml salicylic acid (SA, 1 mM), 50 mg TiO_2 and desired amount (50–300 μl) of various AuNPs suspension under UV irradiation (125 W Hg-arc lamp, 10.4 mW/cm^2 and λ_{max} = 253.6 nm) and magnetic stirring for different time periods at 30 °C temperature. The unreacted SA was measured by UV–vis spectrophotometer (at λ_{max} = 298 nm) and HPLC (C18 column, 50% CH_3OH) analysis. The details of various Au nanostructures are given in supporting information. Zeta potential measurement was done by using Brookhaven Instrument corporation 90plus/BI-MAS instrument. The solution containing Au–SNS (200 μl) or TiO_2 (200 μl form 50 mg per 5 ml water suspension) and water (1.3 ml) was taken in a cuvette for the zeta potential measurement. Similarly, 200 μl of the reaction mixture (1 mM–5 ml SA + 50 mg TiO_2 + 100 μl Au–SNS) was added to 1.3 ml of water and analyzed for surface charge measurement.

3. Results and discussion

The SP band is the most important characteristic property of Au nanoparticles to identify its shape and size. The interaction of light with the Au nanoparticle results in the oscillating electric field which causes the conduction-electrons to oscillate in resonance with the light's frequency coherently and develop the SP resonance. The resonance condition is determined from absorption and scattering spectroscopy and is found [32] to depend on the shape, size, and dielectric constants of both the metal and the surrounding material. Fig. 1 showed the characteristic [33–35] SP bands 530, 563 and 590 nm for Au–SNS, and Au–MNS and Au–LNS nanosphere of three different particle size, respectively. The characteristic [32,33] SP bands 535 and 657 nm are seen for transverse and longitudinal absorption band of Au–NR, respectively. As the shape or size of the nanoparticle changes, the surface geometry changes that led to a shift in the electric field density on the surface. This causes a change in the oscillation frequency of the electrons, generating different cross-sections for the optical properties including absorption and scattering. Chemical aggregation of Au–MNS (563 nm) by CH_3OH addition leads to the evolution of a red-shifted typical SP band at 974 nm along with a band at 557 nm. This has been demonstrated [30,31] to the formation of linear coagulation of AuNPs in polar CH_3OH which was absent on the addition of non-polar (CCl_4) solvent. Table 1 displayed the different physical and optical properties of these various Au nanostructures. The TEM images in Fig. 2a reveal that the average size of the monodisperse Au–SNS is 3.5 ± 0.25 nm (see supporting information) corresponding to SP band 530 nm which is found to be red-shifted as compare to broad absorption band at 520 nm of Au nanosphere [35] having size range 3.5 ± 0.7 nm. It has been also reported [35] that the Au nanospheres of size range between 3.5 and 37 nm exhibit SP bands within 520–530 nm. The evolution of such red-shifted and intense absorption peak of these small Au nanoparticles in our study can be attributed to the improper nucleation and growth of spherical shape particles. In fact, the TEM image of Fig. 2a does not show perfect spherical particles that may change the resonance condition/absorption of light during interaction with electromagnetic radiation. Hence, the apparent reason for highly red shifted SP band compared to the expected value for size <10 nm Au NPs in water might be due to shape and/or aggregation effects of the Au NPs. Similarly, the AuNS size corresponding to SP band 563 nm and 590 nm is expected to be about 80–100 nm as reported [35,36] elsewhere

Table 1
Physical and optical properties of various Au nanostructures.

S. No.	Various Au nanostructures	Measured SP band	Average size (particles considered)	Expected size	Surface area	Surface to volume ratio
1.	SNS	530 nm	3.5 ± 0.25 nm (20)	3.5–37 nm (Ref. 35)	333.44 nm^2	1.95 nm^{-1}
2.	MNS	563 nm	–	80–100 nm (Ref. 33)	–	
3.	LNS	590 nm	9.5 ± 0.06 nm (10)		2058.61 nm^2	0.629 nm^{-1}
4.	PAP	–	6–10 mm (8)	–	–	–
5.	ANS	557 and 974 nm	10–20 nm (12)	–	–	–
6.	NR	535 and 657 nm	Aspect ratio: 2.8 ± 0.12 (12)	–	757.80 nm^2	0.54 nm^{-1}

which is not obtained in our case. Although the size of Au–MNS is not determined, but the size of Au–LNS (SP band 590 nm) is measured to be 9.5 ± 0.06 nm (see supporting information) as shown in the TEM images of Fig. 2b. It seems that the particles are slightly elongated, hence the progressive red shift is observed with increasing the particle size due to their anisotropic shape. The TEM images in Fig. 2c revealed that AuNRs formed are in growth stage and do not show uniform size and shape. The average length, 23.6 nm and aspect ratio, 2.8 ± 0.12 of AuNR are (Fig. 2c) formed along with some cubical shape crystals. It is observed (Fig. 2d) that coagulated chain like assembly of Au–MNS (>5 nm) is formed by CH_3OH addition. It was interpreted [30,31] by the effect of strong dipole–dipole interactions of asymmetrically distributed charges on AuNPs surface in polar solvents and the existence of dipole moments can lead to the linear assembly of AuNS. Aggregated Au deposits (black) of size ranging 6–10 nm are seen (Fig. 2e) onto TiO_2 (gray) after Au (0.02 wt%) photodeposition. Fig. 2f showed the Au nanorods attachment to TiO_2 particles due to the electrostatic interaction between the two colloidal particles in suspension.

Fig. 3 showed the influence of Au co-catalysts size on the PCA of TiO_2 by the addition of 100 μl (~0.02 wt% of TiO_2) Au–SNS, Au–MNS and LNS where ratio of TiO_2 particles to Au atoms (12,500:1) was kept same (see supporting information). It is observed that with decreasing size of AuNPs from 9.5 nm to >5 nm and 3.5 nm, the SA photodegradation rate (PDR) is rapidly enhanced in comparison to bare TiO_2. During SA photodegradation, the Au–SNS exhibited highest PCA, whereas Au–MNS of size >5 nm and Au–LNS of size ≈9.5 nm imparted nearly similar co-catalytic efficiency to TiO_2. Although the added AuNS and TiO_2 are not permanently connected, it is presumed that an electrostatic interaction due to intrinsic surface charge of colloidal particles may occur which facilitate the conduction of photoexcited electron from TiO_2 to AuNS and thereby, increased the PDR by valence band holes. It has been found that the measured zeta potential 50.32 mV for Au–SNS and −2.80 mV

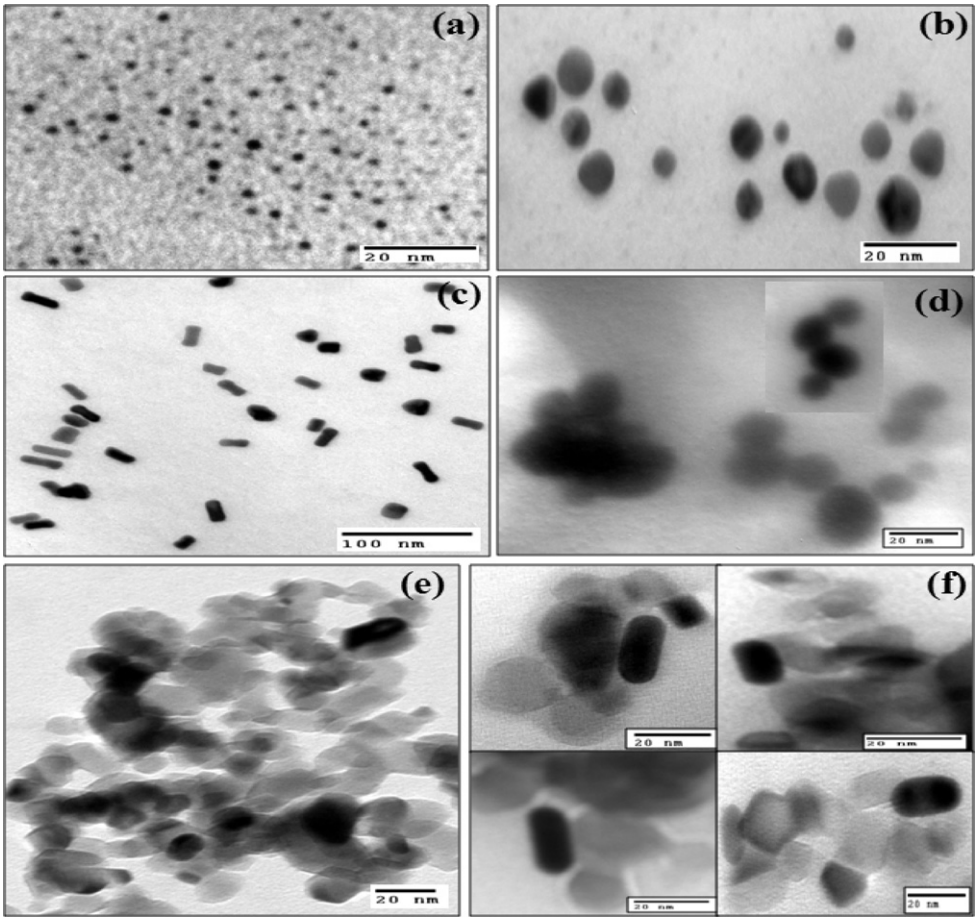

Fig. 2. TEM images of (a) Au small nanospheres, SNS, (b) Au large nanospheres, LNS, (c) Au nanorod, NR, (d) coagulated chain like Au nanospheres, ANS, (e) 0.02 wt% Au photodeposited, PAP onto TiO_2 and (f) Au nanorod, NR-TiO_2 nanoassembly.

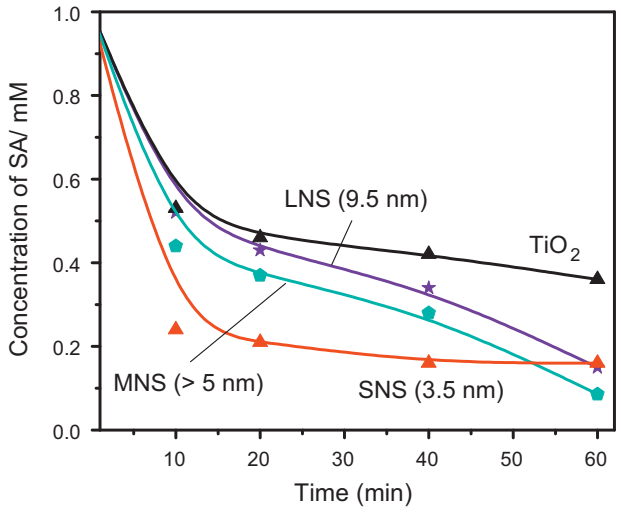

Fig. 3. Effect of loading Au (0.02 wt%) co-catalysts of different sizes on the photocatalytic activity of TiO_2.

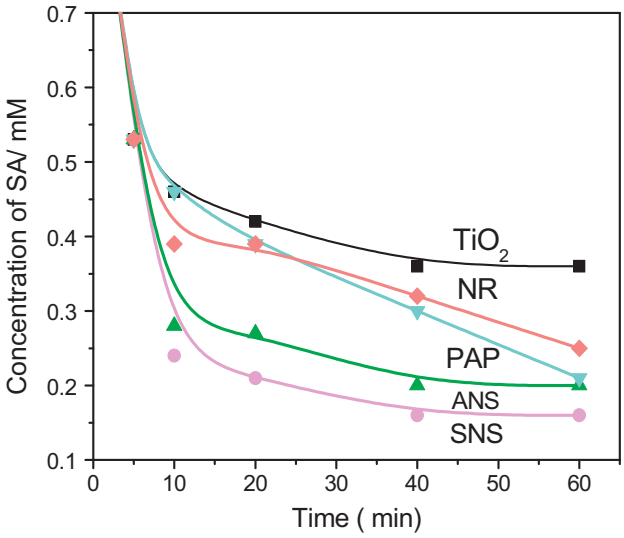

Fig. 5. Comparative rate of salicylic acid photodegradation by different alignments of Au (0.02 wt%)–TiO_2 photocatalysts.

for TiO_2 aqueous solution is reduced to a value of 30.34 mV after mixing them. This fact indicates surface charge neutralization in some extent due to electrostatic interaction between the two unlike nanoparticles. Similar trend is also observed in the experimental reaction mixture of Au–SNS, TiO_2 and salicylic acid. Otherwise, the improvement of PCA would not have been possible if the AuNPs are not in good electrical contact to TiO_2 or separated from each other by an insulating medium.

Fig. 4 displayed the changes of absorption intensity of SA (1 mM, absorption = 2.78 a.u.) during its photooxidation by the addition of 100 μl AuNPs of different morphology to TiO_2 suspension under 1 h light irradiation. Smallest Au–SNS addition almost completely degrades SA (abs. 0.35) as compared to the lowest (abs. 0.86) photoactivity of bare TiO_2. The AuNR loading exhibited lower PCA (abs 0.69) of TiO_2 than the Au–PAP (abs. 0.47) and ANS (abs. 0.50) deposition. The effect of various attachments of Au co-catalysts onto TiO_2 for the degradation of SA for different time periods was shown in Fig. 5. The degradation rate was found to be higher in first 10 min because of the strong adsorption of salicylic acid due to chemisorption at the TiO_2 particle interface forming [37,38] inner-sphere titanium(IV)-salicylate surface complex. This is supported by the

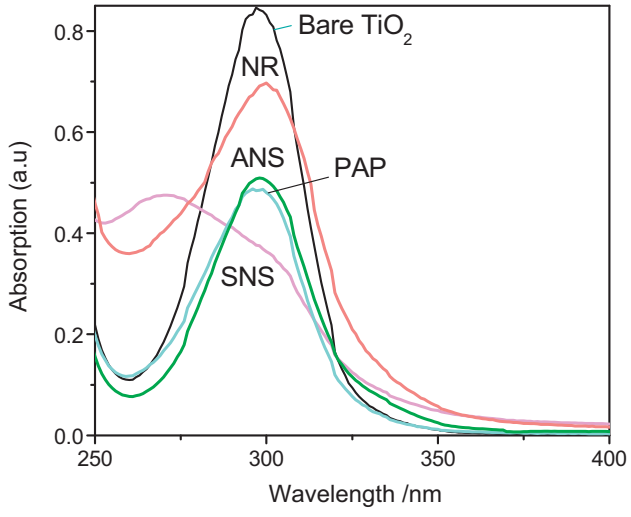

Fig. 4. Changes in absorption spectra of salicylic acid (1 mM, abs: 2.78) during 1 h photodegradation by bare TiO_2 and different Au (0.02 wt%)–TiO_2 nanostructures.

fact that the conductance of Au–SNS (1673 μS) and TiO_2 (57 μS) aqueous solution is highly reduced to 19 μS (experimental reaction mixture) after SA (263 μS) addition due to the complexation through negative charges of —COOH and —OH groups attachments to TiO_2 surface. The PDR of SA is gradually improved after the loading of NR, PAP, ANS and SNS AuNPs onto TiO_2 photocatalyst. The Au–ANS and PAP displayed lower PDR in comparison to the bare quantum size Au–SNS addition. One can observed that the Au–NR loaded TiO_2 significantly retarded the PDR of SA as compared to highly active Au–SNS (≈3.5 nm) loading. This may be due to the constraint of charge accumulation and mobility of the photoexcited electrons in Au–NR for having lesser S/V ratio (0.54 nm^{-1}) than Au–SNS (1.95 nm^{-1}, supporting information). There is a exponential (1st order reaction, $C = C_0\, e^{-kt}$) decrease in SA concentration with reaction time in all the systems which is a characteristic of first order reaction. The PDR of SA is very less after 20–60 min reactions and SA does not completely degraded even after 3 h light irradiation, indicating the photooxidation process [38] follows the first order rate law. Chemisorption, surface charge and thermal catalysis of various Au nanoparticles may also influence the TiO_2 reactivity during initial hours of light irradiation. The average surface area per particles of Au–SNS, Au–LNS and Au–NR are found to be 333.44, 2058.62 and 757.8 nm^2, respectively, (see supporting information) and their co-catalytic activity does not follow the same order. However, their S/V ratio are gradually decreased as 1.95 (Au–SNS) > 0.629 (Au–LNS) > 0.54 nm^{-1} (Au–NR) can reasonably explain the impartment of decreasing co-catalytic activity to TiO_2 catalyst along with the shape effect. The quantum yield of SA degradation at the maximum emission line, 253.6 nm of Hg arc lamp has been found to improve from 0.67% of bare TiO_2 to 0.9% upon Au–SNS (3.5 nm) loading. The photooxidation of SA due to only 253.6 nm UV exposure is verified to be insignificant as compared to photoirradiated bare TiO_2 catalyst. Hence, the fluctuation in the PCA of TiO_2 can be interpreted [21–26] due to the effect of large variation in S/V ratio and difference in percentage of surface active atoms of AuNPs of different size and shape because the amount (0.02 wt%) of Au loading is kept the same. As a result, the diverse rate of photoinduced charge transfer processes took place at the unlike nature of Au–TiO_2 nanojunctions. In fact, because of the high electronegativity of AuNPs, the Fermi level can be shifted to more negative potentials as a function of its different size and shape [20,21]. Thereby, the equilibration of the Fermi-level between the AuNPs and TiO_2, favours electron

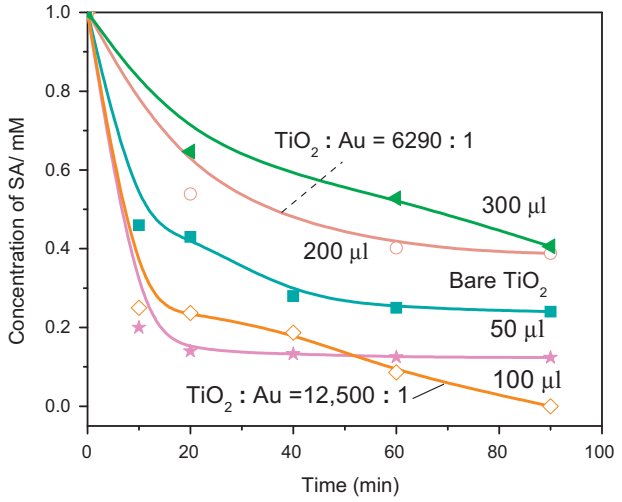

Fig. 6. Effect of varying amount of Au nanosphere (SNS, size ≈ 3.5 nm) addition on the photodegradation rate of 1 mM salicylic acid by TiO_2.

accumulation over small Au nanocrystals, hence, the photoexcited hole could be liberally utilized for the enhanced photooxidation. This was supported [39,40] by the results of higher photocurrent, photovoltage and increasing charge separation as found in the Au–TiO_2 nanostructures. Moreover, Wood et al. [20] also proved the substantial electron accumulation on the Ag, Au, and Cu islands during metal–ZnO photocatalysed reactions.

Fig. 6 showed the influences of varying amount of Au–SNS loading on PCA of TiO_2. It is observed that upto certain concentration (ca. 50–100 µl = 0.01–0.02 wt%) of AuNPs, addition, the PDR is highly increased and thereafter gradually reduced with the increasing (>100 µl) amount of Au–SNS loading as compared to bare TiO_2 activity. Above the optimum (>0.02 wt%) AuNPs (Au–SNS, Au–LNS, AuNR, Au–PAP, ANS), the PCA decreases because once negatively charged, AuNPs become attractive [25,26] for hole, recombine with photogenerated electron in large extent. The presence of large number of electron rich AuNPs and same concentration of photoexcited TiO_2 in the reaction mixture, the recombination rate is probably enhanced because of the increase in frequency of interaction with decreasing ratio (12,500:1 to 6290:1) of TiO_2 to Au atom. Rather than facilitating charge transport and reducing the charge recombination, the Au–SNS may act as the electron–hole recombination centre and retards the quantum efficiency. Moreover, the presence of large number of AuNPs may also slow down mass transport and reduce the PDR. Hence, the optimum amount of metal loading is always beneficial for the maximum photoactivity of TiO_2.

4. Conclusion

The TiO_2 photoactivity has been found to be drastically enhanced with the decreasing size (9.5–3.5 nm) of AuNPs loading. It is interesting to know that the effective amount (0.01 wt%) of Au atom required for maximum PCA of TiO_2 is 100 times less than the traditional prerequisite of 1–2 wt% metal deposition. The AuNR, ANS and PAP addition considerably decreased the PCA of TiO_2 due to the difference in their co-catalytic efficiency that depend on the percentage of surface active atoms and Fermi energy shifts because of the notable change in their size, shape and S/V ratio. The AuNR may lower the substrate adsorption and hinder the direct light absorption on the oxide surface and thus reduced the photogeneration of charged species and the photoactivity. Moreover, the surface area/charge and zeta-potential measurements of each Au–TiO_2 junction of different conformations and the effects of aspect ratio of AuNR loading onto TiO_2 photoactivity are needed to investigate for better understanding the relative co-catalytic activity of various Au nanostrucutres.

Appendix A. Supplementary data

Supplementary data associated with this article can be found, in the online version, at doi:10.1016/j.molcata.2011.11.022.

References

[1] M.I. Litter, Appl. Catal. B: Environ. 23 (1999) 89.
[2] P.V. Kamat, J. Phys. Chem. B 106 (2002) 7729.
[3] M. Murdoch, G.I.N. Waterhouse, M.A. Nadeem, J.B. Meston, M.A. Keane, R.F. Howe, J. Llorca, H. Idriss, Nat. Chem. 3 (2011) 489.
[4] A.J. Bard, M.A. Fox, Acc. Chem. Res. 28 (1995) 141.
[5] S. Ikeda, N. Sugiyama, B. Pal, G. Marci, L. Palmisano, H. Noguchi, K. Uosaki, B. Ohtani, Phys. Chem. Chem. Phys. 3 (2001) 267.
[6] Z. Kasarevic-Popovic, D. Behar, J. Rabani, J. Phys. Chem. B 108 (2004) 20291.
[7] P.V. Kamat, Chem. Rev. 93 (1993) 267.
[8] M. Bellardita, M. Addamo, A.D. Paola, L. Palmisano, Chem. Phys. 339 (2007) 94.
[9] X. Chen, S.S. Mao, Chem. Rev. 107 (2007) 2891.
[10] J. Li, Y. Yamada, K. Murakoshi, Y. Nakatoa, Chem. Commun. 2170 (2001).
[11] P.D. Cozzoli, E. Fanizza, R. Comparelli, M.L. Curri, A. Agostiano, J. Phys. Chem. B 108 (2004) 9623.
[12] C.Yogi, K. Kojima, T. Hashishin, N. Wada, Y. Inada, E.D. Gaspera, M. Bersani, A. Martucci, L. Liu, T.K. Sham, J. Phys. Chem. C 115 (2011) 6554.
[13] J. Lee, W. Choi, J. Phys. Chem. B 109 (2005) 7399.
[14] M.C. Hidalgo, M. Maicu, J.A. Navío, G. Colón, Catal. Today 129 (2007) 43.
[15] M. Haruta, Catal. Today 36 (1997) 153.
[16] J.D. Grunwaldt, C. Kiener, C. Wögerbauer, A. Baiker, J. Catal. 181 (1999) 223.
[17] S. Eustis, M.A. El-Sayed, Chem. Soc. Rev. 35 (2006) 209.
[18] M. Haruta, Chem. Rec. 3 (2003) 75.
[19] A. Schatz, O. Reiser, W.J. Stark, Chem. Eur. J. 16 (2010) 8950.
[20] A. Wood, M. Giersig, P. Mulvaney, J. Phys. Chem. B 105 (2001) 8810.
[21] V. Subramanian, E.E. Wolf, P.V. Kamat, J. Am. Chem. Soc. 126 (2004) 4943.
[22] J. Zeng, Q. Zhang, J. Chen, Y. Xia, Nano Lett. 10 (2010) 30.
[23] R. Narayanan, M.A. El-Sayed, Nano Lett. 4 (2004) 1343.
[24] C. Burda, X. Chen, R. Narayanan, M.A. El-Sayed, Chem. Rev. 105 (2005) 1025.
[25] M. Mrowetz, A. Villa, L. Prati, E. Elena Selli, Gold Bull. 40 (2007) 154.
[26] R. Narayanan, M.A. El-Sayed, J. Phys. Chem. B 109 (2005) 12663.
[27] J. Kimling, M. Maier, B. Okenve, V. Kotaidis, H. Ballot, A. Plech, J. Phys. Chem. B 110 (2006) 15700.
[28] B. Nikoobakht, M.A. El-Sayed, Chem. Mater. 15 (2003) 1957.
[29] X. Huang, S. Neretina, M.A. El-Sayed, Adv. Mater. 21 (2009) 4880.
[30] J. Liao, Y. Zhang, W. Yu, L. Xu, C. Ge, J. Liu, N. Gu, Colloids Surf. A: Physicochem. Eng. Aspects 223 (2003) 177.
[31] J.H. Liao, K.J. Chen, L.N. Xu, C.W. Ge, J. Wang, L. Huang, N. Gu, Appl. Phys. A 76 (2003) 541.
[32] K. Lance Kelly, E. Coronado, L.L. Zhao, G.C. Schatz, J. Phys. Chem. B 107 (2003) 668.
[33] L.M. Liz-Marzan, Langmuir 22 (2006) 32.
[34] W. Ni, X. Kou, Z. Yang, J. Wang, ACS NANO 2 (2008) 677.
[35] N.R. Jana, L. Gearheart, C.J. Murphy, Langmuir 17 (2001) 6782.
[36] W. Haiss, N.T.K. Thanh, J. Aveyard, D.G. Fernig, Anal. Chem. 79 (2007) 4215.
[37] A.E. Regazzoni, P. Mandelbaum, M. Matsuyoshi, S. Schiller, S.A. Bilmes, M.A. Blesa, Langmuir 14 (1998) 868.
[38] J.A. Anderson, Catal. Today 175 (2011) 316.
[39] Y. Nakato, K. Ueda, H. Yano, H. Tsubomura, J. Phys. Chem. 92 (1988) 2316.
[40] V. Subramanian, E. Wolf, P.V. Kamat, J. Phys. Chem. B 105 (2001) 11439.